Late Stages in the Evolution of Low and Intermediate Mass Stars

Garrelt Mellema

April 21, 2008

1 Introduction

This part of the course treats the post-Main Sequence (post-MS) evolution of stars. The most massive stars (above $\sim$9 $M_\odot$) will end their lifes as supernovas, and were treated in the first part of this course. Here we will consider the stars with an initial mass (Zero Age Main Sequence or ZAMS mass) of less than 9 $M_\odot$, who will end their lifes as White Dwarfs.
Stars evolve due to irreversible processes. The two main irreversible processes in stars are

1. nuclear burning (in the central regions)
2. mass loss (from their surface)

In the classical theory of stellar evolution (before the 1980s) only the first of these processes was taken into account. In absence of mass loss, the division between supernova- and white dwarf-producing stars would lie at $M_{\rm ZAMS} \simeq$4 $M_\odot$, when the core reaches the Chandrasekhar mass (1.4 $M_\odot$). The fact that this line in reality lies at a twice higher mass already indicates the central role mass loss plays in stellar evolution. Because of uncertainties in the description of the mass loss processes, the actual theoretical dividing line remains somewhat uncertain, but lies somewhere in the range 8–10 $M_\odot$.
Supernovae are spectacular events, but why are lower mass stars important?

- Most stars are low mass stars; so they form an essential part of stellar populations.
- Source of material processed in nuclear burning (chemical enrichment), as well as source of dust.
- Our own Sun is a low mass star, so we are studying its future.
- Interesting (astro)physics and chemistry (complex molecules, including organic molecules).

The Main Sequence (MS) evolution time of a star depends on the stellar mass according to $t_{\rm evol} \propto M^{-2.5}$. This means in practice that a 8 $M_\odot$ star will reach the end of its evolution in 50 Myr, and a 0.8 $M_\odot$ star in 14 Gyr. The latter have therefore not had the time to evolve off the MS within the life of the Universe (13.6 Gyr).
The empirical Salpeter Initial Mass Function (IMF) for stellar populations gives

$$\frac{{\rm d}N}{{\rm d}M} \propto M^{-2.35} \tag{1}$$

which means that of a coeval stellar population, 96% of the stars have a mass between 0.8 and 8 $M_\odot$.
The post-Main Sequence evolution of stars with $M_{\rm ZAMS} < 9$ $M_\odot$ goes through the following stages

1. Red Giant Branch (RGB) phase
2. Horizontal Branch (HB) phase

3. Asymptotic Giant Branch (AGB) phase
4. Planetary Nebula (PN) phase
5. White Dwarf phase

The emphasis of these lectures will be on the AGB phase, which together with the PN phase is the area of most active research worldwide, and also in Sweden (Stockholm, Onsala, Uppsala). Areas that are being actively investigated are for example

- Mass loss and circumstellar material (CSM)
- Pulsations and variability
- Metal production
- Transition of AGB stars into PNe.

2 Basic Stellar Evolution

Essentially all detailed information we have about stellar evolution comes from numerical simulations. In their simplest form these simulations apply a slow evolution to the 1D equations of (static) stellar structure:

$$\text{Mass conservation:} \tag{2}$$

$$\frac{\mathrm{d}M_r}{\mathrm{d}r} = 4\pi r^2 \rho \tag{3}$$

$$\text{Hydrostatic equilibrium:} \tag{4}$$

$$\frac{\mathrm{d}p}{\mathrm{d}r} = -\frac{GM_r\rho}{r^2} \tag{5}$$

$$\text{Energy production:} \tag{6}$$

$$\frac{\mathrm{d}L_r}{\mathrm{d}r} = 4\pi r^2 \rho\epsilon \tag{7}$$

$$\text{Energy transport:} \tag{8}$$

$$\frac{\mathrm{d}T_r}{\mathrm{d}r} = \begin{cases} -\frac{3}{4ac}\frac{\bar{\kappa}\rho}{T^3}\frac{L_r}{4\pi r^2} & \text{if } \frac{\mathrm{d}\ln P}{\mathrm{d}\ln T} > \gamma/(\gamma-1) \text{ (radiative diffusion)} \\ -\left(1-\frac{1}{\gamma}\right)\frac{\mu m_{\mathrm{H}}}{k_{\mathrm{B}}}\frac{GM_r}{r^2} & \text{if } \frac{\mathrm{d}\ln P}{\mathrm{d}\ln T} < \gamma/(\gamma-1) \text{ (adiabatic convection)} \end{cases} \tag{9}$$

combined with

$$\text{Equation of state:} \quad p = p(\rho, T, \text{composition}) \tag{10}$$

$$\text{Opacity:} \quad \bar{\kappa} = \bar{\kappa}(\rho, T, \text{composition}) \tag{11}$$

$$\text{Nuclear reactions:} \quad \epsilon = \epsilon(\rho, T, \text{composition}) \tag{12}$$

where M_r is the interior mass ($M(< r)$), L_r the interior luminosity, μ the mean molecular weight and γ the polytropic index (for example 5/3 for a monatomic gas and 4/3 for a relativistic gas).

The equations for hydrostatic equilibrium and mass play a rather passive role in this set of equations. For stellar evolution the interesting things happen in the processes of energy production (ϵ) and transport ($\mathrm{d}T/\mathrm{d}r$).

We will now look at the results of two calculations by John Lattanzio, one for $M_{\mathrm{ZAMS}} = 1$ M$_\odot$ (low mass star, Fig. 1) and one for $M_{\mathrm{ZAMS}} = 5$ M$_\odot$ (intermediate mass star, Fig. 3).

2.1 A 1 $M_\odot$ star

On the Main Sequence, the energy production stars less massive than 1.3 $M_\odot$ is dominated by the proton-proton chain (Fig. 2), which has a relatively mild dependence on temperature ($\epsilon_{\mathrm{pp}} \propto T^4$), and therefore the core will use radiative energy transport. This has an effect that the H abundance decreases and the He abundance increases 'inside-out' (see inset a), giving a smooth transition from nuclear H burning in the core to H shell burning around the He-core (at point 4).

As the inactive He-core grows through the addition of He from the H burning shell, it contracts, and the envelope expands. The densities in the He-core become high enough

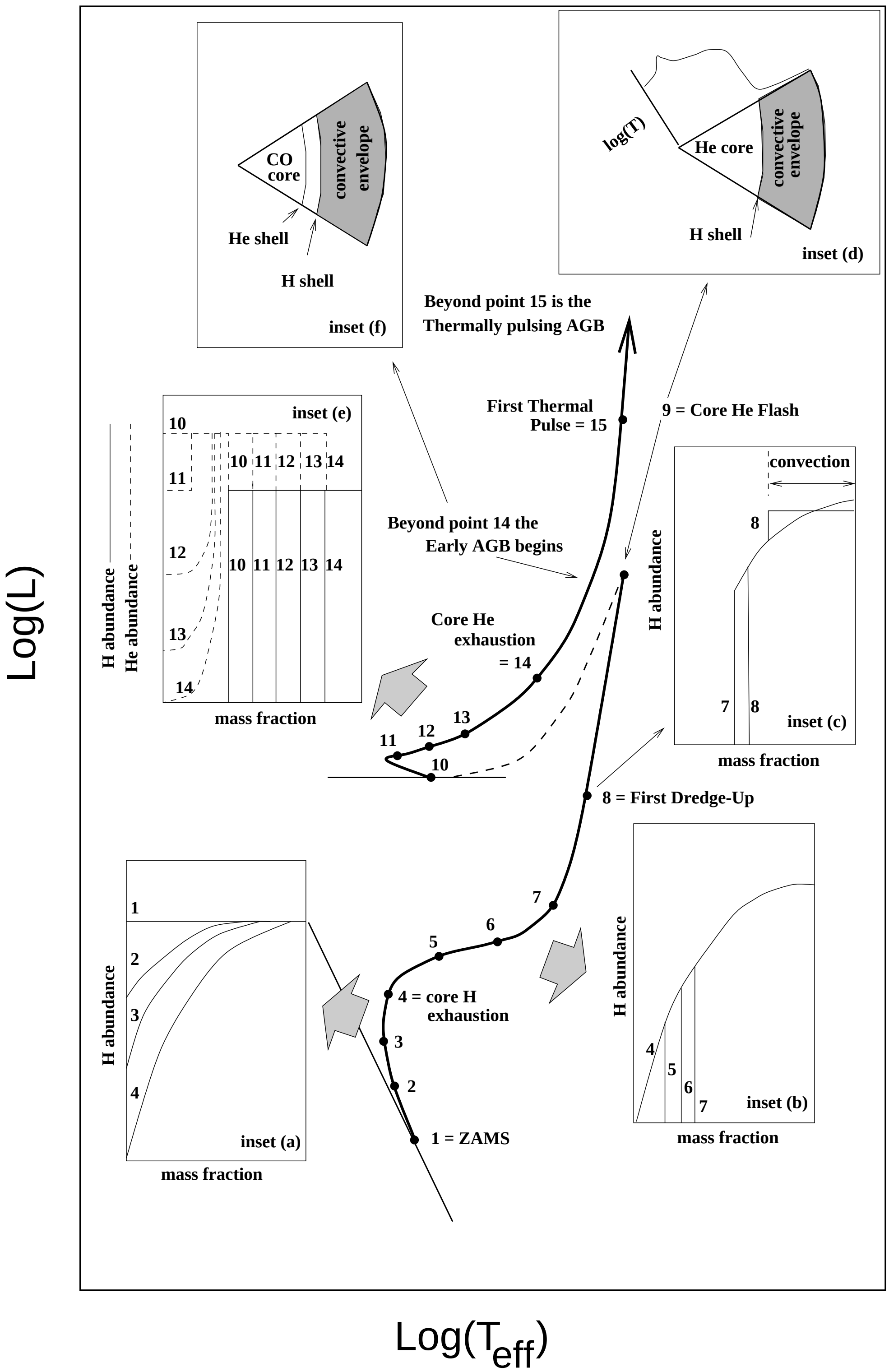

Figure 1: Schematic evolution of a 1 $M_{\odot}$ star across the HR diagram. From Lattanzio & Wood (2004).

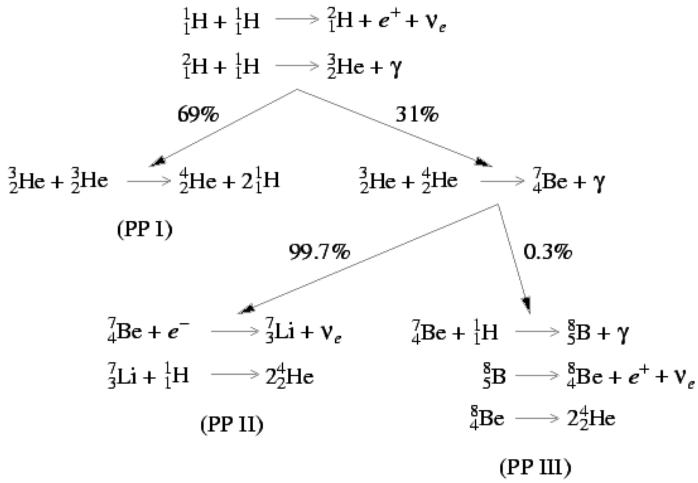

Figure 2: The proton-proton chain

for the electrons to become degenerate, after which the pressure of the material is only a function of density, no longer of temperature (points 4–7).

As the star approaches the Hayashi limit (point 7), its envelope becomes fully convective and it evolves at nearly constant $T_{\rm eff}$, while increasing its luminosity L (and hence its radius R). This phase is the ***Red Giant Branch*** (RGB). During this phase the convection may reach the H burning shell and mix up processed material into the stellar envelope. This process is known as the ***First Dredge Up*** (point 8). Its chemical signature is as follows: (^{4}He $\uparrow$, ^{14}N $\uparrow$, ^{12}C $\downarrow$, ^{12}C/^{13}C $\downarrow$).

The RGB ends when He-fusion starts in the core (point 9). He-fusion occurs through a process known as the 3α process, which has a strong temperature dependence ($\propto T^{40}$). If the core is (electron) degenerate ($M_{\rm ZAMS} < 2.3$ M$_\odot$), He-fusion starts with a runaway process known as the Helium Flash. However, nearly all of the energy generated in the Helium Flash is used to rearrange the internal structure of the star, and so the flash itself is not observable.

In the next phase known as the ***Horizontal Branch*** phase (points 10–14), the star has He-core burning and H-shell burning. The He-core burning produces ^{12}C with the 3α process. The ^{12}C can react further via ^{12}C(α,γ)^{16}O to form a ^{12}C/^{16}O core. The rate of this last reaction is uncertain, so the final ratio between ^{12}C and ^{16}O in the core is also uncertain.

During this phase, the inner core is convective, but the outer core is semi-convective, leading to a smooth transition from He-core burning to He-shell burning, which is the start of the AGB (point 14).

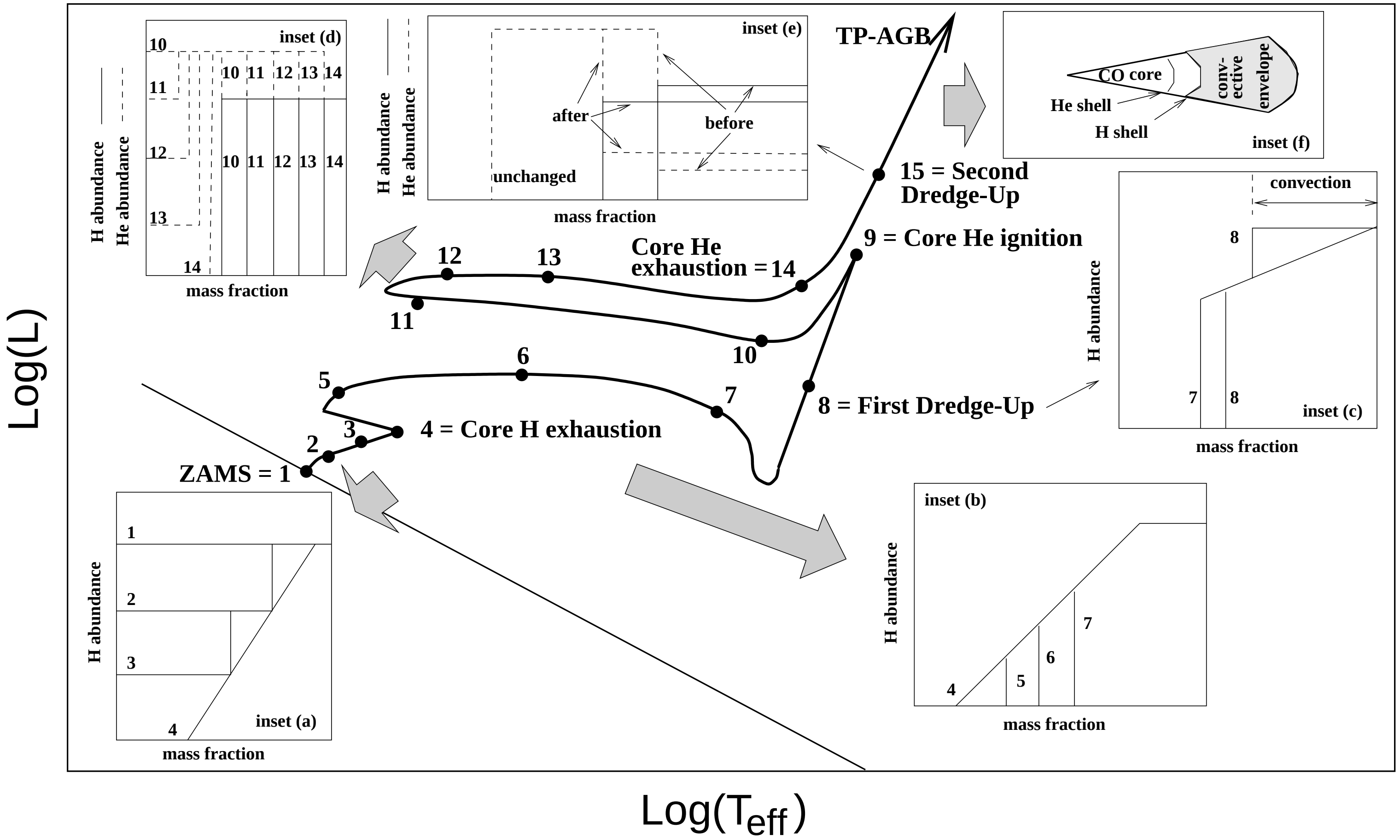

Figure 3: Schematic evolution of a 5 $M_\odot$ star across the HR diagram. From Lattanzio & Wood (2004).

$$
\begin{array}{ccc}
{}^{12}C + {}^{1}H & \rightarrow & {}^{13}N + \gamma \\
{}^{13}N & \rightarrow & {}^{13}C + e^{+} + \nu_e \\
{}^{13}C + {}^{1}H & \rightarrow & {}^{14}N + \gamma \\
{}^{14}N + {}^{1}H & \rightarrow & {}^{15}O + \gamma \\
{}^{15}O & \rightarrow & {}^{15}N + e^{+} + \nu_e \\
{}^{15}N + {}^{1}H & \rightarrow & {}^{12}C + {}^{4}He \\
{}^{15}N + {}^{1}H & \rightarrow & {}^{16}O + \gamma \\
{}^{16}O + {}^{1}H & \rightarrow & {}^{17}F + \gamma \\
{}^{17}F & \rightarrow & {}^{17}O + e^{+} + \nu_e \\
{}^{17}O + {}^{1}H & \rightarrow & {}^{14}N + {}^{4}He
\end{array}
$$

Figure 4: The CNO cycle reactions

2.2 A 5 $M_\odot$ star

On the Main Sequence these stars have H-core burning through the CNO-cycle (Fig. 4). This process has a stronger temperature dependence than the pp-chain, which leads to a convective core. Because of this the H-concentration drops homogeneously through the core region (Fig. 3, inset a), and the end of H-core burning occurs suddenly (point 4).
At this point the core is heavier than the so-called Schönberg-Chandrasekhar limit

$$\frac{M_{\rm core}}{M} > 0.4 \left(\frac{\mu_{\rm env}}{\mu_{\rm core}}\right)^2 \sim 0.1 \tag{13}$$

and therefore contracts rapidly (points 4-5). This leads to the ignition of H-shell burning (point 5), and further rapid core contraction ('Herzsprung gap', points 5-7). Upon reaching the RGB, also in these stars the first dredge-up takes place (point 8).
He-core burning starts without a flash, since the core is not electron-degenerate (point 9).
During the HB both the He-core and H-shell are active. Their relative strengths determine how high $T_{\rm eff}$ becomes. There is no semi-convective outer core for this type of star. When He-shell burning starts (point 14), the star enters the AGB phase.

2.3 Mass limits

There are a number of useful mass limits to keep in mind.

$$\text{Main Sequence: } M_{\rm ZAMS} \begin{cases} < 1.3 M_\odot & \text{pp-chain dominates} \\ > 1.3 M_\odot & \text{CNO-cycle dominates} \end{cases}$$

$$\text{RGB: } M_{\rm ZAMS} \begin{cases} < 2.3 M_\odot & \text{electron-degenerate He-core} \\ > 2.3 M_\odot & \text{non-degenerate He-core} \end{cases}$$

$$M_{\rm ZAMS} < 0.6 M_\odot \quad \text{He-burning never starts}$$

$$M_{\rm ZAMS} \begin{cases} < 9 M_\odot & \text{electron-degenerate C/O core} \\ > 9 M_\odot & \text{non-degenerate C/O core} \end{cases}$$

The last division is interesting. In principle the start of C-burning in a degenerate core will lead to a C-flash, which would be powerful enough to disrupt the core and star, leading to a thermonuclear supernova. Because mass loss reduces the mass during the RGB/AGB phases, these type of supernovae may not exist. Thermonuclear supernova do of course occur when White Dwarfs due to external processes reach the Chandrasekhar mass, leading to the famous type Ia supernovae.

2.4 Shell sources

We end this introductionary section with a review of some of the properties of shell sources, which are important both during the early and late post-MS evolution. When nuclear burning occurs in a shell, the physics imposes certain restrictions.

The shell source is associated with a density jump. The reason for this is that the pressure and the temperature at the core–shell interface should be constant (to have hydrostatic and thermal equilibrium), but the composition and the thus the mean molecular weight of the core and shell material differ. Since the pressure, density and temperature are related through the ideal gas law

$$p = \frac{\rho k_{\rm B} T}{\mu m_{\rm H}}\,, \tag{14}$$

a jump in μ implies a jump in ρ. For example, if the core is 100% He, it will have $Y = 1$, giving $\mu_{\rm core} = 4/3$. Is the shell has 30% He, it will have $X = 0.7$, $Y = 0.3$, and $\mu_{\rm shell} = 0.62$. This then implies $\rho_{\rm core} = 2.2 \times \rho_{\rm shell}$.

The shell source position remains approximately fixed in space. The cause is a negative feedback loop involving the strongly non-linear temperature dependence of the nuclear fusion processes. If the shell acquires a smaller radius, its temperature will go up. Therefore its energy production will go up enormously, increasing the pressure of the shell, making it expand, thus increasing its radius, and lowering the temperature again. For example, for a 1 $M_\odot$, $r_{\rm shell} = 0.03\ R_\odot$ throughout the RGB phase.

Shell sources reverse the contractive/expansive behaviour of the layers below them. When a core contracts, it in fact does not homologously contract, but instead becomes more highly concentrated towards its centre, thus increasing the density gradient (since $r_{\rm shell}$ is roughly constant). This causes the stellar envelope to expand. Note that this is a real expansion, since the stellar radius can be changed. The actual physical cause for this reversal behaviour is still being debated, but the effect can clearly be seen in stellar evolution models. There are two easy rules of thumb for this:

- Core contraction [active shell] Envelope expansion
- Core expansion [active shell] Envelope contraction

So the active shell source can be said to mirror the behaviour of the inner regions.

3 Stellar Evolution during the AGB Phase

Both low- and intermediate mass type stars actually reach the AGB with similar internal structures:

- C/O core (degenerate)
- He-shell
- Intershell region
- H-shell
- H-envelope

As we will see in more detail later, the He-shell is thermally unstable, leading to periodic He-shell flashes, also known as thermal pulses. The phase before the first thermal pulse is known as the Early-AGB (E-AGB), the phase thereafter (starting at point 15 in Fig. 1 and 3) is known as the thermally pulsing AGB (TP-AGB).
During the E-AGB stars of initial mass $M_{\rm ZAMS} > 4M_\odot$ temporarily lose their H-burning shell. This allows envelope convection to reach into the region of partially burnt H, and mix up processed material in what is known as the second dredge-up (^{4}He $\uparrow$, ^{12}C $\downarrow$, ^{13}C $\uparrow$, ^{14}N $\uparrow$).
On the TP-AGB the evolution of low and intermediate mass stars is qualitatively similar, being characterized by

- A sequence of He-shell flashes, with longer interpulse periods during which the H-shell dominates the energy production.
- Extensive mass loss from the stellar surface ($> 10^{-7}\ M_\odot$ yr^{-1}...).

Since the typical luminosity of an AGB star is in the range 10^3–$10^4\ L_\odot$, one can estimate that the star needs to burn $\sim 10^{-8}\ M_\odot$ yr^{-1} to produce this luminosity. This means that during the AGB phase, the stellar evolution is dominated by mass loss rather than by nucleosynthesis!
The internal structure of AGB stars is extremely inhomogeneous (see Fig. 5). For example for a 1 $M_\odot$ star

	$q = m_r/M$	$R(R_\odot)$
He-shell	0.516	0.017
H-shell	0.560	0.035
Surface	1.0	225 (~ 1 AU)

This implies that

$$\rho_{\rm core} \sim 10^5 \text{ g cm}^{-3}$$
$$\rho_{\rm envelope} \sim 10^{-7} \text{ g cm}^{-3}$$

To appreciate these number we can compare them to the density of the Earth atmosphere ($\sim 10^{-3}$ g cm^{-3}).
In what follows we will look closer at the following aspects

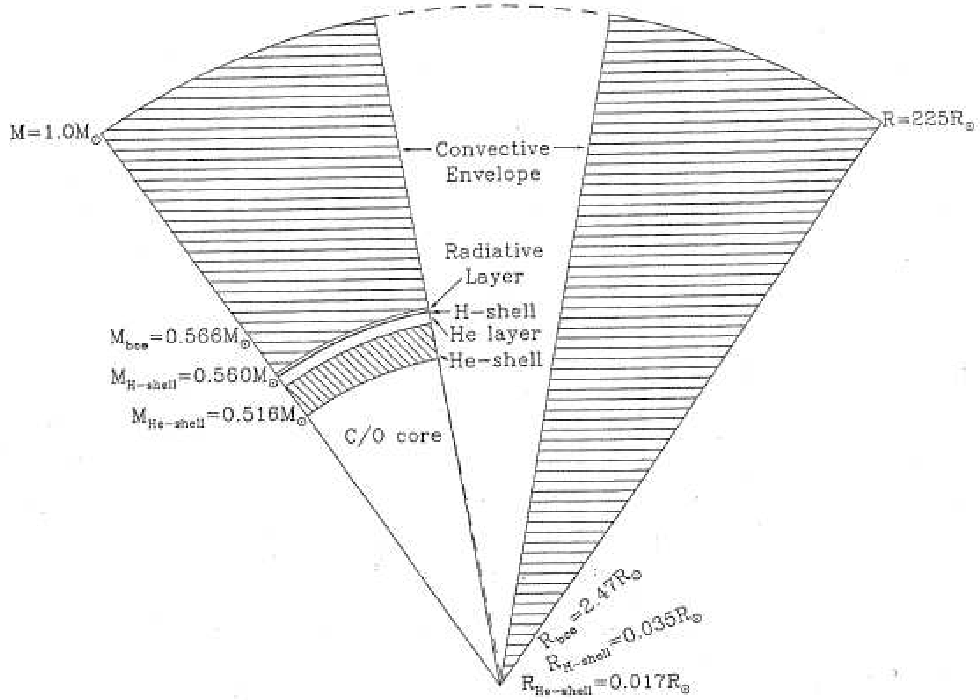

Figure 5: A schematic view of a 1 $M_\odot$ AGB star interior. On the left, various regions are plotted against mass fraction, while on the right the regions are plotted against radius. $M_{\rm bce}$ is the mass at the base of the convective envelope, while $M_{\rm H-shell}$ and $M_{\rm He-shell}$ are the masses at the middle of the hydrogen- and helium-burning shells, respectively. From Lattanzio & Wood (2004).

- Thermal pulses, nuclear synthesis and dredge-up (Sect. 4)
- Stellar pulsations (Sect. 5)
- Mass loss and the structure of the circumstellar envelope (Sects. 6 and 7)
- Post-AGB evolution (Sect. 8)

4 Thermal Pulses, Nuclear Synthesis, and Dredge-Up

Thermal pulses are brief periods of runaway He burning in the He-shell of an AGB star. In the interpulse periods the active H-shell produces He which is added to the inactive He-shell. Above a certain shell mass the He-shell ignites and makes a He-shell flash. The first question to ask is why this is a runaway process.

4.1 Gravothermal specific heats

The thermal evolution of a pocket of gas is given by

$$\frac{\mathrm{d}T}{\mathrm{d}t} = \frac{1}{C}\frac{\mathrm{d}q}{\mathrm{d}t}\,, \tag{15}$$

where C is the specific heat, and q is the specific energy added or removed. If C includes the gravitational effects (work done by the pocket of gas), it is called the gravothermal specific heat, C_*. From hydrostatic equilibrium and basic thermodynamics it can be shown that

$$C_* = C_p\left(1 - \nabla_{\mathrm{ad}}\frac{4\delta}{4\alpha-3}\right)\,, \tag{16}$$

where α and δ are given by the equation of state (EOS) of the gas: $\rho \propto p^{\alpha}T^{-\delta}$ and ∇_{ad} is the adiabatic temperature gradient

$$\nabla_{\mathrm{ad}} = \left(\frac{\mathrm{d}\ln p}{\mathrm{d}\ln T}\right)_S\,. \tag{17}$$

The derivation of this expression can be found in Ciardullo's lecture notes (lecture 20). For a monatomic gas $\nabla_{\mathrm{ad}} = 2/5$ and $\alpha = 1$, $\delta = 1$. This means that $C_* < 0$ for such a gas. The effect is that adding heat to a region causes a drop in temperature. This may seem counterintuitive, but is due to the fact that adding heat will make the region expand, requiring work since the surrounding gas has to be pushed away, which thus lowers the temperature. This also means that if such a pocket of gas has nuclear reactions, it will be stable against small perturbations: adding small amounts of heat will reduce the temperature, and hence reduce the energy production by nuclear reactions (which are strongly temperature-dependent). In other words there is a negative feedback loop.

For a (non-relativistically) electron-degenerate gas $\alpha = 3/5$ and $\delta = 0$, making C_* positive: adding heat will make the temperature go up. Consequently, the pocket will be unstable when nuclear processes are active, since the rise in temperature will increase the energy production, which will increase the temperature even more, a positive feedback loop.

However, in a star energy can also be carried away by radiation, so for a more complete analysis we also need to include the effect of energy transport by radiation. As can be seen from the equations of stellar structure, the efficiency of energy transport by radiation is inversely proportional to the opacity κ of the gas. The opacity will be a function of the gas density and temperature

$$\kappa \propto \rho^{p}T^{q} \tag{18}$$

We also need to consider the energy production rate ϵ which also depends on the density and temperature

$$\epsilon \propto \rho^{\lambda} T^{\nu} \tag{19}$$

Some algebra (Ciardullo, lecture 20) shows that when including the effect of opacity, the rate of change for the temperature can be written as

$$\frac{\mathrm{d}T}{\mathrm{d}t} = \frac{K}{C_*}\frac{\mathrm{d}T}{T} \tag{20}$$

with

$$K = \frac{L}{M}\left[(\nu + q - 4) + \frac{\delta}{4\alpha - 3}(3\lambda + 3p + 4)\right] \tag{21}$$

where L and M are the luminosity and mass of the region under consideration (the stellar core or a shell source). For the pp-chain $\nu = 4$ and $\lambda = 1$, for Kramer's opacity $p = 1$ and $q = -3.5$, so using an ideal monatomic gas gives a positive K together with a negative C_*, resulting in a negative feedback loop, and a stable nuclear burning region.

For the He-burning 3α process, $\nu = 40$ and $\lambda = 2$, so for an electron degenerate gas starting He-fusion both K and C_* are positive, leading to positive feedback and the He-core flash.

Now how does this work for a shell source? First of all it is important to realize that the derivation for C_* that led to Eq. 16 assumed a spherical region which could expand in all directions. If r is the size of the region, its volume is $\frac{4}{3}\pi r^3$ and a change $\mathrm{d}r$ in size leads to a change in volume

$$\mathrm{d}V = \frac{3}{r}V\mathrm{d}r \tag{22}$$

However, a shell cannot expand in all directions. If we have a thin shell of thickness D at radial position r, its volume is $4\pi r^2 D$, and its change of volume when increasing its thickness by $\mathrm{d}D$ is

$$\mathrm{d}V = \frac{1}{D}V\mathrm{d}D = \frac{r}{D}\frac{V}{r}\mathrm{d}D \tag{23}$$

This means that the factor 3 in Eq. 16 has to be replaced by r/D

$$C_*^{\mathrm{shell}} = C_p\left(1 - \nabla_{\mathrm{ad}}\frac{4\delta}{4\alpha - r/D}\right) \tag{24}$$

For a monatomic gas $\alpha = 1$, so if $D < r/4$ then $C_* > 0$ and the shell will be unstable! So even when the gas is non-degenerate (which it will be outside of the core), nuclear burning in shells can be unstable. The physical reason is that for a thin shell, a small change in D will cause a large change in the density ρ, but only a very small change in r, so not much energy is used in the expansion of the shell, leading to insufficient energy loss due to expansion, and thus a positive gravothermal specific heat. The instability is quenched when by expanding the shell becomes thick enough to break the $D < r/4$ condition.

The conclusion is that shells with active nuclear burning have to be relatively thick, but inactive shells can of course be thin. However, upon starting nuclear fusion, the process will be unstable, leading to a shell flash. This is exactly what happens to the He-shell in AGB stars.

4.2 Interpulse times

Numerical modelling of the thermal pulse process with stellar evolution codes shows that the time between these events is

$$\log \tau_{\rm p} = 4.5(1.678 - \frac{M_{\rm core}}{M_\odot}) \qquad \text{(years)} \tag{25}$$

For a 1 $M_\odot$ star with a core mass of 0.6 $M_\odot$ this means an interpulse time of 70,000 years, whereas for a 5 $M_\odot$ star with a core mass of 1 $M_\odot$, $\tau_{\rm p} = 1100$ years.
Since during a He-shell flash a lot of energy is released in a short time, the region around the C/O core is modified. The peak luminosity can be as high a 10^9 $L_\odot$. This leads to a number of interesting and important effects, caused by convective mixing and nucleosynthesis, effects that due to convective dredge-up even affect the surface layers of the star.

4.3 Anatomy of a thermal pulse

A thermal pulse cycle consists of a number of phases, which we will now describe qualitatively. See also Fig. 6.

Off the He-shell is dormant and produces almost no energy. The main source of energy is the H-shell. This state is the one which takes most of the time in a cycle. For stars with $M \gtrsim 3$ $M_\odot$ the convective envelope reaches down to the H-shell ('Hot Bottom Burning', see later). For lower mass stars the envelope is radiative just above the H-shell (which leads to the luminosity-core mass relation, see later).

On The He-shell ignites, $L \sim 10^8$–10^9 $L_\odot$. A convective zone develops above the He-burning zone ('intershell convective zone' or 'intershell region', ISR). This convection transports up ^{4}He and He-fusion products (^{12}C). This phase lasts 10–100 years (depending on core mass).

Power-down The energy production in the He-shell declines, but the energy it produced drives an expansion of the ISR, pushing the H-shell outward, so that it also extinguishes. In this phase there is no, or very little energy production, and it also lasts some 10–100 years.

Dredge-up The transport of the energy produced in the shell flash starts convection in the envelope, reaching all the way down into the ISR, mixing up material that was involved in He-burning (e.g., ^{12}C). This phase also lasts typically some 10–100 years.

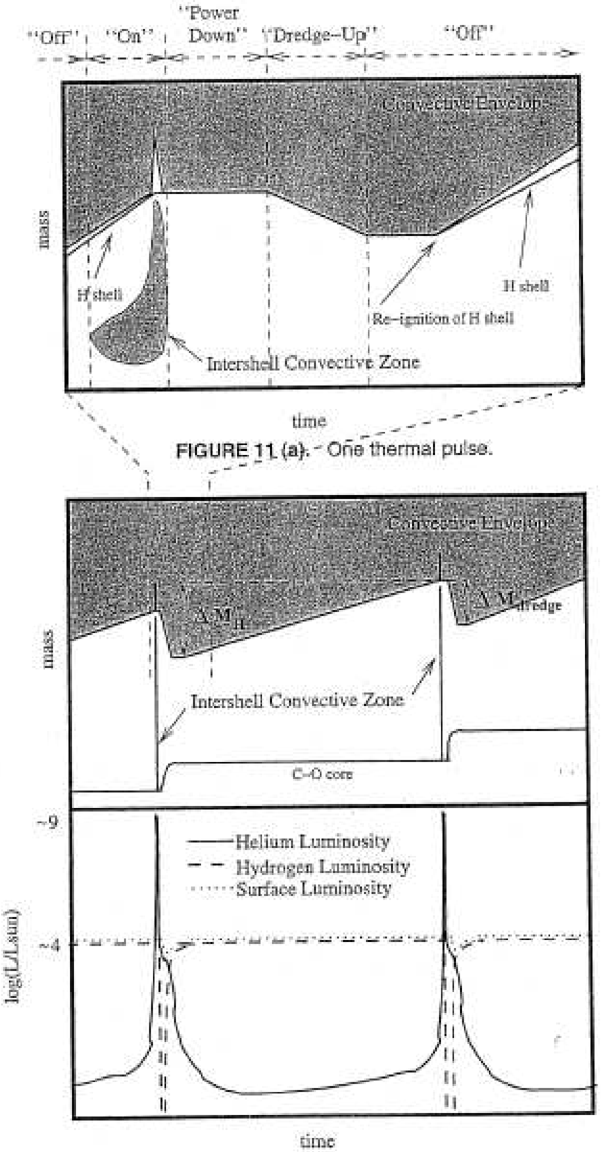

Figure 6: Some details of the interior evolution during one thermal pulse (top) and for two consecutive pulses (bottom). Convective regions are shaded. The line toward the bottom of the middle panel shows the position of the He-burning shell ($Y = 0.5$). The position of the H-burning shell is indistinguishable from the position of the base of the convective envelope in this panel. The "On", "Power-down", "Dredge-Up" and "Off" phases of the thermal pulse cycle are marked on the top panel.

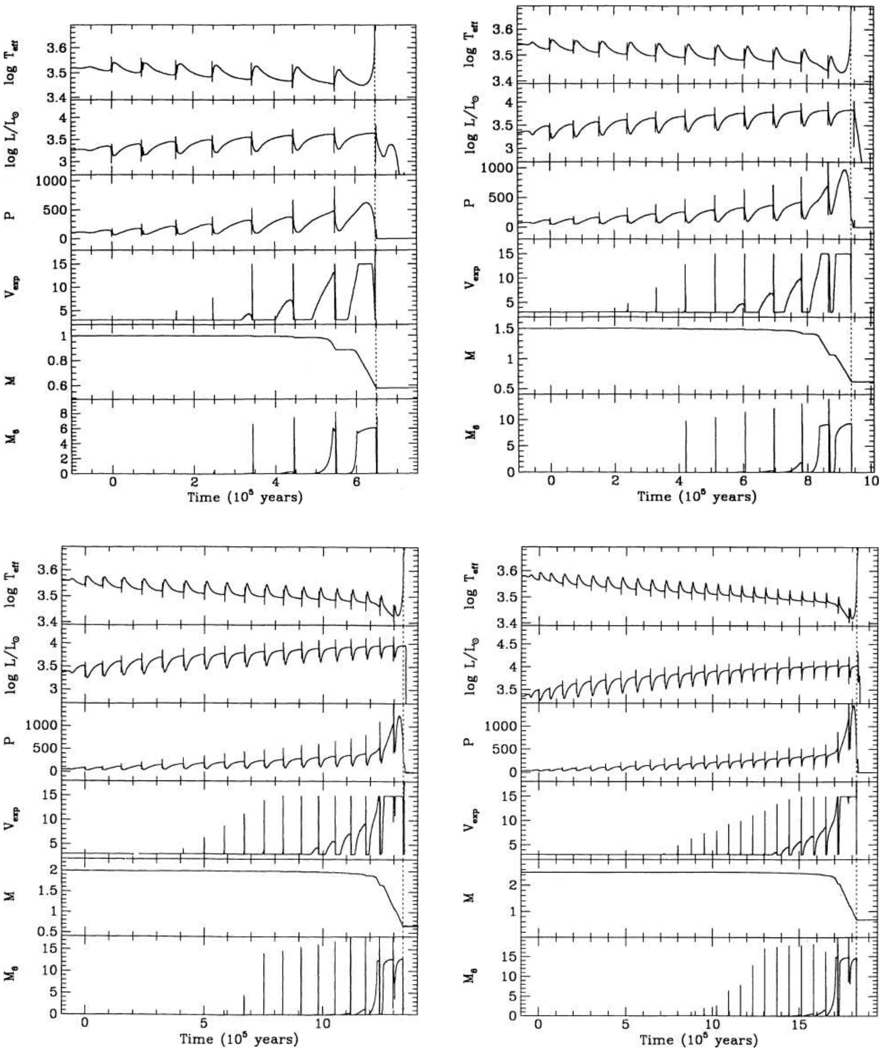

Figure 7: Time dependence of various quantities during the TP-AGB phase of stars with $(Y, Z) = (0.25, 0.008)$ and masses 1 (top left), 1.5 (top right), 2 (bottom left), 2.5 $M_\odot$ (bottom right). The abscissa represents the time after the first major thermal pulse. The dotted vertical line at the right represents the end of the AGB phase. M_6 is the mass loss rate in units of $10^{-6} M_\odot$ yr^{-1}. From Vassiliadis & Wood (1993).

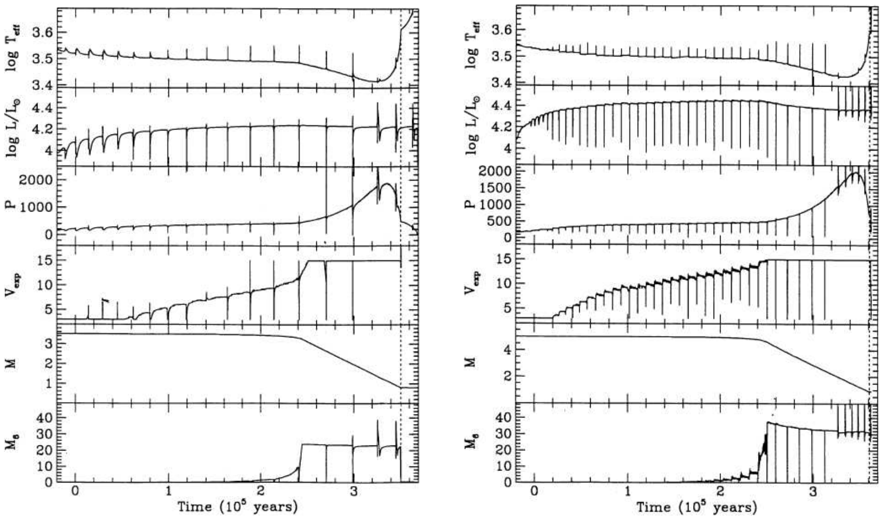

Figure 8: As Fig. 7 but for masses 3.5 (left) and 5 $M_{\odot}$ (right).

4.4 Evolution on the TP-AGB

During the TP-AGB phase the star will experience a series of thermal pulses of the type described above. The total number of thermal pulses depends on the duration of the entire AGB phase, which as we have seen above depends on the mass loss from the surface. Numerical simulations show typical numbers of 10 (for a 1 $M_{\odot}$ star) to 40 (5 $M_{\odot}$). See Figs. 7 and 8 showing the evolution of a number of stellar parameters during the TP-AGB for six different initial masses.
Just as in the case of the He-core flash, the luminosity produced in the He-shell flash does not reach the surface of the star, at least not initially. But as the envelope mass is reduced by mass loss, for later pulses a short luminosity increase does become visible (see Fig. 12). However, the drop in luminosity during the "Power down" phase always becomes visible at the stellar surface.
As can be seen in the Figs. 7 and 8 other stellar parameters such as the effective temperature and pulsation period also vary during the thermal pulse cycle.

4.5 Core mass-Luminosity Relation

During the TP-AGB the luminosity in the "off" phase keeps going up. This can be expressed as the core mass-luminosity relation

$$L_{\rm AGB} = 5.9 \times 10^4 (M_{\rm c} - 0.52) \qquad L_{\odot} \tag{26}$$

(Paczynski 1970). This relation is due to the fact that the envelope essentially has zero pressure compared to the electron-degenerate C/O core, making its presence irrelevant for the energy producing core region. Various more or less equivalent CMLRs have been found in stellar evolution models (see Fig. 9)

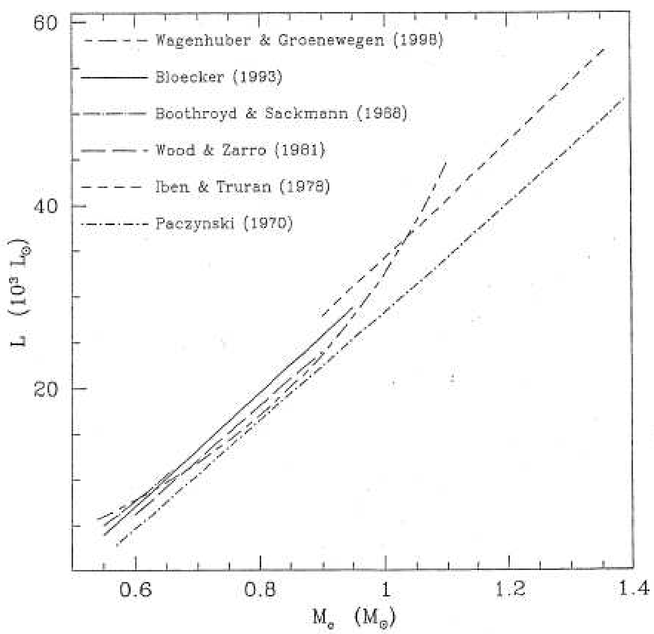

Figure 9: Core mass-Luminosity Relations from various authors, each plotted in the range of M_{c} considered to obtain the analytical fit to the model results. When a composition dependence is present, the solar case is considered, i.e. ($Z = 0.02$, $Y = 0.28$). The relation by Iben & Truran (1978) refers to a 7 $M_{\odot}$ model.

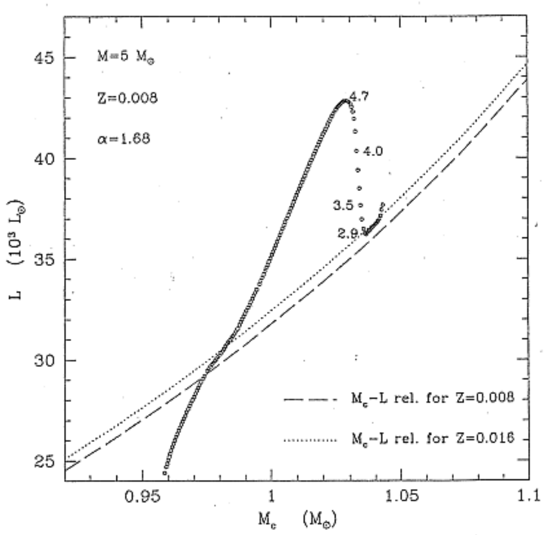

Figure 10: Luminosity evolution of a 5.0 $M_\odot$, $Z = 0.008$ star experiencing HBB. The open circles correspond to the maximum quiescent luminosity before each thermal pulse. The numbers along the curve indicate the current stellar mass in solar units. The dashed and dotted lines represent the reference CMLR for $Z = 0.008$ and $Z = 0.016$ respectively. From Marigo (1998).

L–M_c relations exist for all giant phases, but for the RGB phase are of the type $L \propto M_\mathrm{c}^8$. For AGB stars this becomes the linear relation $L \propto M_\mathrm{c}$ due to the domination of radiation pressure (see Ciardullo, lectures 21 and 24).
Because of the L–M_c relation one can find limits for the luminosity during the AGB:

$$\begin{aligned} \text{AGB: } & L_\mathrm{min} \approx 2800 L_\odot \\ & L_\mathrm{max} \approx 51000 L_\odot \\ \text{RGB: } & L_\mathrm{max} \approx 2900 L_\odot \end{aligned}$$

The lowest luminosity AGB stars are thus almost indistinguishable from the highest luminosity RGB stars. The position of the tip of the RGB is sometimes used to estimate the distance to nearby galaxies. Contamination by AGB stars is thus a worry. It is harder to use the tip of the AGB for this since this phase lasts so much shorter, and thus is less populated in a Herzsprung-Russell diagram.
The L–M_c relation on the AGB breaks down for the more massive stars, as in those the base of the envelope gets involved in the energy production. This is known as Hot Bottom Burning (HBB). Figure 10 shows how the luminosity evolution of a 5 $M_\odot$ deviates from the CMLR, until HBB stops due to the reduced mass of the stellar envelope and the star joins the CMLR.

4.6 Hot Bottom Burning

This is the process of H-burning at the bottom of the convective envelope. This only occurs above a certain stellar mass ($\sim 5\ M_\odot$ for $Z = Z_\odot$, lower at lower metallicity). The process stops when the envelope has lost too much mass.
HBB burning breaks the L–M_c relation, and so massive AGB stars do not follow this relation, as can be seen in Fig. 10.
HBB also leads to interesting nucleosynthesis products since convective motions carry away intermediate products of H-burning (CNO and pp-chain). In steady regions of nuclear processing these products are processed further, and never contribute to chemical enrichment, but as HBB happens at the base of the convective envelope these products may be mixed up into the envelope and change the surface abundances.
Take for example ^{7}Li:

$$^3\mathrm{He} +^4 \mathrm{He} \rightarrow^7 \mathrm{Be} + \gamma$$
$$^7\mathrm{Be} + e^- \rightarrow^7 \mathrm{Li} + \nu$$

Both ^{7}Be and ^{7}Li can react with ^{1}H, but outside the area of nucleosynthesis this will not happen. So, if one produces ^{7}Be in HBB and mix it up, it has a large chance of capturing an electron and producing ^{7}Li. The stellar sources and sinks of ^{7}Li are important to understand, as this is one of the elements that was formed in small quantities during the Big Bang. Measurements of the ^{7}Li can thus constrain cosmological models, but only if one can estimate what stellar processes produce and destroy it.

4.7 Dredge Up

During thermal pulses, material from deep down the shells can be dredged up into the stellar convective envelope, and thus cause abundance changes even at the stellar surface. The dredge up during thermal pulses is also known as the 3rd dredge up (3DUP), as similar events happen on the RGB and during the E-AGB (the latter only for massive enough stars).
The efficiency of dredge-up is usually expressed by a parameter

$$\lambda = \frac{\Delta M_\mathrm{dredge-up}}{\Delta M_\mathrm{c}} \tag{27}$$

where

$\Delta M_\mathrm{dredge-up}$ Mass dredged up into the envelope.

ΔM_c Growth of core mass between two thermal pulses.

For low mass stars $\lambda \lesssim 0.3$, and for stars initially more massive than $\sim 5\ M_\odot$, $\lambda \lesssim 1$. However, these numbers are very uncertain.

4.7.1 Carbon Stars

The most dramatic effect of the 3rd dredge up is the transformation of AGB stars from M-type stars into C-type stars (Carbon stars). The cosmic and solar abundance ratio

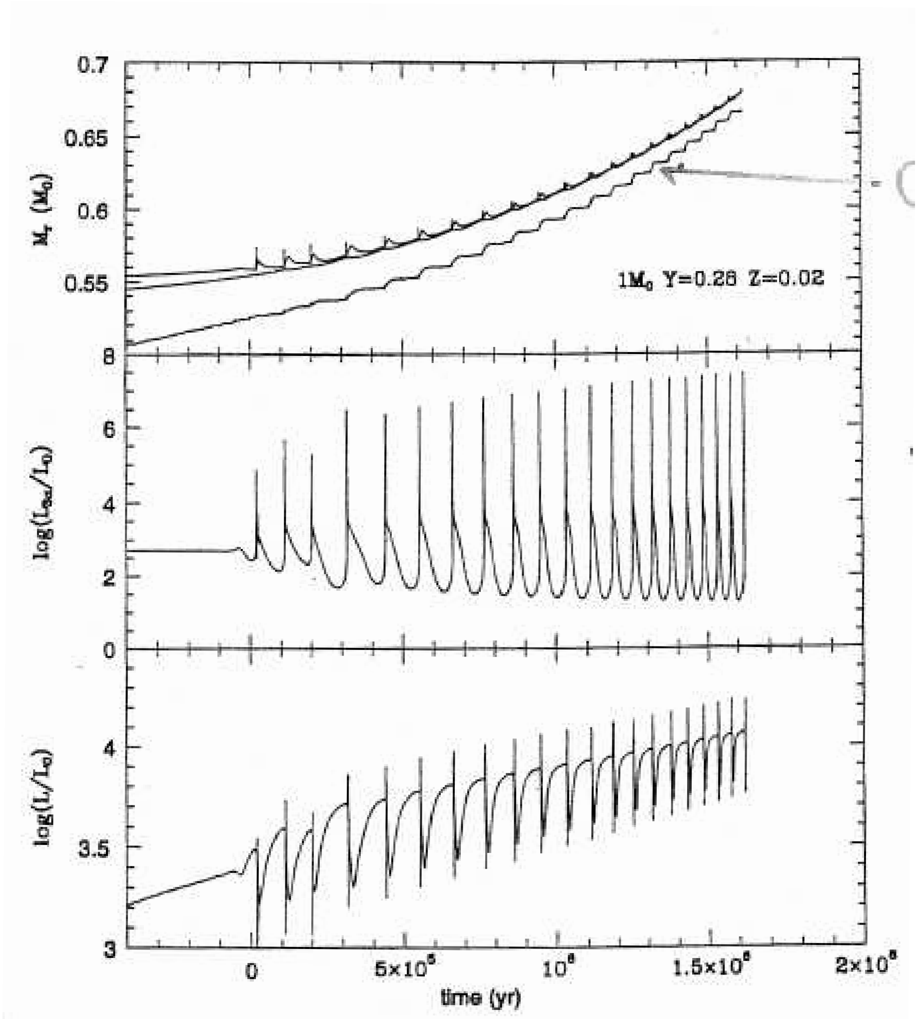

Figure 11: Plots of (from top to bottom) the core masses, He-luminosity and total luminosity as a function of time for a 1 $M_\odot$. The core masses shown are the mass of He-exhausted core, the H-exhausted core, and the base of the convective envelope.

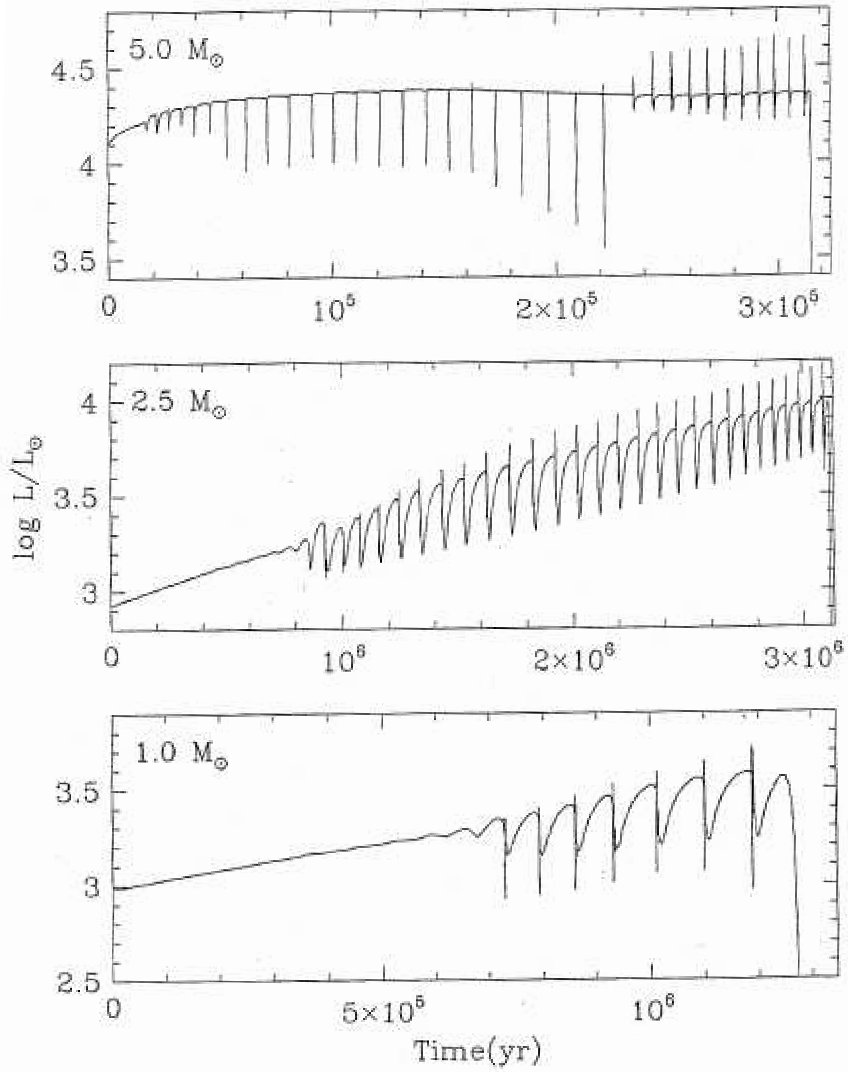

Figure 12: The surface luminosity evolution of thermally pulsing AGB stars of mass1, 2.5 and 5.0 $M_{\odot}$, and initial composition $Y = 0.25$ and $Z = 0.016$. The plots start on the early AGB when the H- and He-burning luminosities are equal and end when the stars have left the AGB and moved to the post-AGB part of the HR-diagram. From Vassiliadis & Wood (1993).

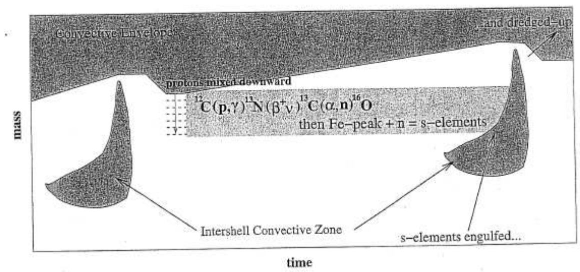

Figure 13: Schematic showing internal evolution between two pulses. Partial mixing during the third dredge-up phase produces a ^{13}C pocket, which provides the neutrons for the s-processing. Note that this figure is not to scale: the protons are mixed downward a depth of only a few $\times 10^{-4} M_{\odot}$, whereas the intershell convective zone is up to a few $\times 10^{-2} M_{\odot}$ in extent.

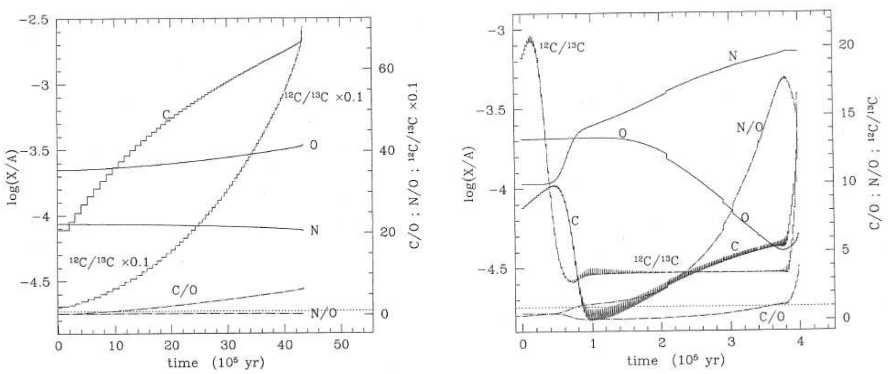

Figure 14: Evolution of CNO surface abundances (by number, mole gr^{-1}) and ratios from the first thermal pulse until the complete ejection of the stellar envelope for a $Z = 0.008$ TP-AGB model with initial mass 2.5 $M_{\odot}$ (left) and 5 $M_{\odot}$ (right). The efficiency factor for the third dredge-up is assumed to be $\lambda = 0.5$; the mixing length parameter is $\alpha = 0.24$. Based on synthetic calculation by Marigo (1998).

between carbon and oxygen is C/O$\sim$ 0.4–0.5. Carbon stars have C/O> 1. This is mostly ^{12}C from the He-burning shell that was dredged up during thermal pulses. The spectrum of Carbon stars differs dramatically from that of M-type stars, mostly because of a number of carbon containing molecules, such as CO and CN.
Careful modelling of this process suggests a minimum mass to form Carbon stars of about 1.5 $M_\odot$. Below this, the stars experience too few thermal pulses and is the dredge up process too weak to turn the star into a Carbon star. There is also a maximum mass, since HBB can remove ^{12}C through the CNO-cycle, by turning it into ^{14}N. This would thus mean that the maximum mass for Carbon stars is $\sim 5\ M_\odot$. Note however that the HBB process switches off at the end of the AGB, so for initially more massive stars there is a chance of becoming a Carbon star quite late in the process. See Fig. 14 for two examples of how the surface CNO abundances change during the AGB.

4.7.2 Other abundance changes

Dredge up not only changes the surface abundances, it also facilitates unusual nuclear reactions, as it mixes primordial, H-burnt and He-burnt material. Convection will carry the products from these reactions to the surface, and as AGB stars lose mass, this makes them the main cosmic producers of some elements/isotopes.

- Dredge up increases ^{12}C, ^{22}Ne, ^{25}Mg, ^{26}Mg
- H-shell and HBB
  - burn ^{12}C and ^{18}O into ^{14}N $\Rightarrow$ ^{14}N$\uparrow$, ^{18}O$\downarrow$
  - burn ^{22}Ne into ^{23}Na $\Rightarrow$ ^{23}Na$\uparrow$
  - produce ^{25}Mg, ^{26}Mg $\Rightarrow$ ^{25,26}Mg$\uparrow$
- More massive stars ($M_{\rm ZAMS} \gtrsim 6 M_\odot$?): ^{24}Mg $\rightarrow$ ^{27}Al $\Rightarrow$ ^{24}Mg $\downarrow$ ^{27}Al $\uparrow$

4.7.3 s-process

In addition, AGB stars produce so-called s-process elements. The s-process is the process of slow neutron capture. Neutron capture is the only way to make elements beyond the Fe peak, since the binding energy per nucleon peaks around Fe. For the s-process, the (negative) β decay should occur more rapidly than the next neutron capture. This way the most stable isotopes at each atomic weight are formed.
The s-process does not produce elements beyond Pb since

$$\begin{aligned}
{}^{209}\mathrm{Bi} + n &\rightarrow {}^{210}\mathrm{Bi} + \gamma \\
{}^{210}\mathrm{Bi} &\rightarrow {}^{210}\mathrm{Po} + e^- + \bar{\nu}_e \\
{}^{210}\mathrm{Po} &\rightarrow {}^{206}\mathrm{Pb} + {}^{4}\mathrm{He} \\
{}^{206}\mathrm{Pb} + 3n &\rightarrow {}^{209}\mathrm{Pb} \\
{}^{209}\mathrm{Pb} &\rightarrow {}^{209}\mathrm{Bi} + e^- + \bar{\nu}_e
\end{aligned}$$

All the heavier elements require the r-process, which operates in supernova explosions.

A special spectral class has been defined for stars with s-process elements in their spectra, the S-type stars. They show for instance lines of ZrO. There are also intermediate types such as MS-stars, which in addition show TiO, and CS-stars which also show C_2 and CN lines. Evolutionary it is inferred that the transition from M-type stars to C-type stars happens as M→MS→S→CS→C, as the s-process elements also are produced in thermal pulses and are being dredged up to the surface. A star with s-process elements in its spectrum is thus on its way to become a C-star (but may not necessarily get there). Some AGB stars show lines of Technitium (Tc), the lightest element without any stable isotopes. The most stable isotope of Tc, ^{99}Tc, has a half life of only 2×10^5 years, thus giving direct evidence for the occurence of the s-process and dredge up.
Although there is good observational evidence for the occurrence of the s-process, how it proceeds inside AGB is stars is not well understood. The problem is that one needs an appropriate source of neutrons. This source is thought to be one (or both) of the following nuclear reactions

$$^{13}\mathrm{C} +^{4}\mathrm{He} \rightarrow^{16}\mathrm{O} + n$$
$$^{22}\mathrm{Ne} +^{4}\mathrm{He} \rightarrow^{25}\mathrm{Mg} + n$$

The second one of these can only operate in higher mass stars since it requires temperature in excess of 3×10^8 K.
Formation of ^{13}C is however, a sensitive process proceeding like

$$^{12}\mathrm{C} + p \rightarrow^{13}\mathrm{N} + \gamma \rightarrow^{13}\mathrm{C} + e^{+} + \nu_e$$

but if many protons are present it will quickly react with them according to

$$^{13}\mathrm{C} + p \rightarrow^{14}\mathrm{N} + \gamma$$

So, to produce enough ^{13}C a limited supply of protons, mixed down from the envelope into the ^{12}C region left behind by the thermal pulse, is necessary. This then so-called ^{13}C pocket would produce the s-process elements, which will be dredged up during the next thermal pulse.